Strong-coupling descriptions of high-temperature superconductors: electronic attraction from a repulsive potential

1993 J. Phys.: Condens. Matter 5 199

(http://iopscience.iop.org/0953-8984/5/2/008)

J. Phys.: Condens. Matter 5 (1993) 199–216. Printed in the UK

Strong-coupling descriptions of high-temperature superconductors: electronic attraction from a repulsive potential

W Barford† and M W Long‡

† Department of Physics, University of Sheffield, Sheffield S3 7RH, UK
‡ School of Physics and Space Research, University of Birmingham, Birmingham B15 2TT, UK

Received 16 July 1992, in final form 9 November 1992

Abstract. We consider the effect of the nearest-neighbour copper–oxygen repulsion, V, when coupled to the charge transfer resonances $Cu^{2+} \rightarrow Cu^{3+}$ and $Cu^{2+} \rightarrow Cu^{+}$ in the high-temperature cuprate superconductors. This is done by deriving effective low-energy Hamiltonians correct to second order in the copper–oxygen hybridization. Only hole doping is considered. When $Cu^{2+} \rightarrow Cu^{3+}$ fluctuations dominate we derive an effective one-band model of 'Zhang–Rice' singlets with a nearest-neighbour repulsion between these singlets. When $Cu^{2+} \rightarrow Cu^{+}$ fluctuations dominate we find rich and complex behaviour. If $0 \ll V/\Delta \leqslant \frac{1}{2}$ (where Δ is the 'bare' copper–oxygen charge transfer gap) we show that clusters of charge are more stable than isolated charges. On the other hand, if $0 \leqslant V/\Delta \ll \frac{1}{2}$ the Hamiltonian contains both weak attractive and repulsive two-body potentials. Calculations on clusters indicate that the attractive potentials have the same correlations as the more dominant 'single-particle' terms suggesting the possibility of 's'-wave pairing.

1. Introduction

An unusual feature of the copper oxide high-temperature superconductors is the close proximity of the atomic copper and oxygen energy levels. This leads to charge transfer resonances of the type $Cu^{2+} \rightarrow Cu^{3+}$ and $Cu^{2+} \rightarrow Cu^{+}$. Varma, Schmitt-Rink and Abrahams [1] were the first to offer general arguments that these charge transfer resonances, coupled to the nearest-neighbour copper–oxygen repulsion, could lead to 's-wave' superconductivity. Numerical [2, 3] and mean-field calculations [4, 5] confirmed that charge clustering and superconducting instabilities are indeed a possibility for certain parameter ranges.

In this paper we address this issue by deriving an effective low-energy Hamiltonian from the natural tight-binding Hamiltonian for the copper-oxide planes [6] which includes the copper and oxygen orbitals on an equal footing. This is

$$H_0 = -\frac{\Delta}{2}\sum_{i\sigma} d^{\dagger}_{i\sigma} d_{i\sigma} + U\sum_{i} d^{\dagger}_{i\sigma} d^{\dagger}_{i\bar{\sigma}} d_{i\bar{\sigma}} d_{i\sigma} + \frac{\Delta}{2}\sum_{j\sigma} p^{\dagger}_{j\sigma} p_{j\sigma}$$
$$+ U_p \sum_{j} p^{\dagger}_{j\sigma} p^{\dagger}_{j\bar{\sigma}} p_{j\bar{\sigma}} p_{j\sigma} + V \sum_{\langle ij\rangle\sigma\sigma'} d^{\dagger}_{i\sigma} d_{i\sigma} p^{\dagger}_{j\sigma'} p_{j\sigma'} \qquad (1.1a)$$

0953-8984/93/020199+18$07.50

$$H_1 = t \sum_{\langle ij \rangle \sigma} (d^\dagger_{i\sigma} p_{j\sigma} + p^\dagger_{j\sigma} d_{i\sigma}) \tag{1.1b}$$

where $d^\dagger_{i\sigma}$ and $p^\dagger_{j\sigma}$ create *holes* in the relevant hybridizing orbitals on copper (site label i) and oxygen (site label j) atoms respectively. The vacuum of (1.1) is the closed shells d^{10} (Cu^+) and p^6 (O^{2-}). Δ is the 'bare' charge transfer gap, t is the hopping matrix element connecting copper and oxygen sites, V is the nearest-neighbour copper–oxygen Coulomb repulsion and the Us are the on-site Coulomb repulsions. Spectroscopic evidence [7] and fittings to constrained density functional calculations [8] suggest that $U \sim 9$ eV, $U_p \sim 5$ eV, $V \sim 0.8$ eV, $\Delta \sim 3$ eV and $t \sim 1.5$ eV. Another term, which is sometimes considered, is the direct oxygen–oxygen hopping matrix element, $t_{pp} \sim 0.6$ eV, which has the effect of renormalizing the charge transfer gap. This term will not be considered in this paper. The 'parent' compound has one hole in every copper orbital (d^9) and empty oxygen orbitals (p^6).

Our approach is to treat t perturbatively, relegate all the other energy scales to zero or infinity and perform a Schrieffer–Woolf canonical transformation [9, 10] on (1.1) in the presence of the nearest-neighbour Coulomb repulsion. This derives an effective Hamiltonian whose leading order hopping term is $O(t^2)$, and where there are residual many-body effects resulting from the copper–oxygen repulsion. The restriction to second order in the hybridization does mean, however, that we cannot include the antiferromagnetic super-exchange effects directly; we therefore only consider the effects caused by the motion of charge carriers. In principle, spin fluctuations can be included on an *ad hoc* basis by adding a Heisenberg term to the effective Hamiltonians.

This method has been used by Fedro and Schüttler [11] and the present authors [12] to derive an effective Hamiltonian for electron doping. In this case the low-energy physics is described by a one-band Hubbard model with a nearest-neighbour repulsion of the charge carriers which reside on the copper sites. In this paper we only consider hole doping. In section 2 the motion of charge carriers via virtual Cu^{3+} excitations is considered. We find that an essentially single-band model describing the motion of the 'Zhang–Rice' singlet [13], with a nearest-neighbour repulsion of these singlets, is appropriate. In sections 3, 4 and 5 a detailed discussion of the motion of charge carriers via virtual Cu^+ excitations is given. We find quite different and very rich behaviour. First, even the motion of a single oxygen hole becomes difficult to analyse, rendering the 'Zhang–Rice' analysis incomplete. Second, when $0 \ll V/\Delta \leqslant \frac{1}{2}$ we find that charge clustering occurs. Third, when $0 \leqslant V/\Delta \ll \frac{1}{2}$ we find evidence from cluster calculations for weak-coupling 's-wave' superconductivity, in agreement with the mean-field analyses [4, 5]. The conclusions of this work have been presented elsewhere [14]. Finally, we conclude this paper in section 6.

2. Motion of holes via Cu^{3+} excitations

In the two-band model (1.1) in the atomic limit there are two natural charge states for the added hole. The first possibility is that the copper sites dominate with the holes forming Cu^{3+}. The second is that both copper and oxygen sites must be considered with the added hole residing on oxygen sites as O^-, and these holes move about in a spin background residing on the copper sites. The second case will only be considered as this is experimentally more justifiable [7]. With the assumption that the holes

reside predominantly on oxygen sites there are still two important limits to consider as the hybridization is increased. If the direct oxygen–oxygen hybridization is small then delocalization occurs across copper sites. There are two distinct mechanisms for hole motion. The first is to assume that added holes hop between oxygen sites via an intermediate state in which the copper site is doubly occupied with holes, namely Cu^{3+}. The second is to assume that in the intermediate state a hole vacates the copper site leaving a closed shell, namely Cu^{+}. The experimental evidence is in favour of the latter, but in this section we consider the former possibility. We treat only virtual occupancy of the intermediate charge states, separating out the two physical effects by allowing the copper Coulomb repulsion, U, to diverge. In this section we enforce this by allowing $\Delta \to \infty$ while $(U - \Delta) < \infty$.

The assumptions that each new d state is singly occupied and that the intermediate state involves the Cu^{3+} gives, by the second-order canonical transformation [9, 10] (details may be found in [12]),

$$H = -t^2 \sum_{\langle ij\rangle\sigma} \sum_{\langle ij'\rangle\sigma} S_{ij}^{\dagger} [f_{ij}^{-1} + f_{ij'}^{-1}] S_{ij'} \tag{2.1a}$$

for the $O(t^2)$ part of the Hamiltonian, with the 'singlet' operator being defined as

$$S_{ij}^{\dagger} = \frac{1}{\sqrt{2}} \sum_{\sigma} \mathrm{sgn}(\sigma) p_{j\sigma}^{\dagger} d_{i\bar{\sigma}}^{\dagger} \tag{2.1b}$$

and the matrix element

$$f_{ij} = U - \Delta - 2V - U_{\mathrm{p}} P_j + V \sum_{\langle ij\rangle} P_l \tag{2.1c}$$

where $P_j = \sum_{\sigma} p_{j\sigma}^{\dagger} p_{j\sigma}$ is the oxygen hole operator.

The form of this description may be readily understood. Since the intermediate state involves two holes on a copper site the relevant oxygen hole must be in a singlet configuration with respect to the copper site that hybridizes with it. The $S_{ij}^{\dagger}$ operators create precisely the relevant spin configuration.

In order to understand the matrix elements, however, we study the states that the 'new' operators create. The $d_{i\sigma}^{\dagger}$ creates a pure copper hole in this limit. The energy gap between this hole and the neighbouring oxygen levels is assumed to be infinite, so the hole gains nothing by hybridizing. The $p_{j\sigma}^{\dagger}$ creates a hole that is predominantly on the oxygen site but is optimally hybridized onto the two neighbouring copper sites. When the 'oxygen' hole resides on an oxygen site it is repelled by both neighbouring copper holes. However, when it resides on a copper site it is repelled by the holes on neighbouring oxygen sites. The first consequence of this repulsion is that doped holes only reside on the oxygen sites provided that $U > \Delta + 2V$, so the nearest-neighbour repulsion tends to push the doped holes onto the copper sites in this limit. The second and more important consequence is that the nearest-neighbour repulsion between the copper and oxygen holes induces a many-body repulsion between charge carriers. This is because when several 'oxygen' holes neighbour the same copper site, partial occupation by one of those holes on the copper site results in a repulsion between that hole and all the other 'oxygen' holes. This is a peculiarity to the topology of the

copper oxide lattice: each copper site has four neighbouring oxygen sites, but each oxygen site has only two neighbouring copper sites.

We may derive the repulsion directly by performing the inversion of the operator f_{ij} (2.1*c*). Since f_{ij} is a sum of commuting operators the inversion is trivial, and a general prescription is derived in the appendix. For the case where $U_p \to \infty$ we find

$$H_1 = -D_1 \sum_{\langle ij \rangle} \sum_{\langle ij' \rangle} S_{ij}^{\dagger} S_{ij'} \tag{2.2a}$$

$$H_2 = D_2 \sum_{\langle ijl \rangle} \sum_{\langle ij'l \rangle} S_{ij}^{\dagger} P_l S_{ij'} \tag{2.2b}$$

$$H_3 = -D_3 \sum_{\langle ijlm \rangle} \sum_{\langle ij'lm \rangle} S_{ij}^{\dagger} P_l P_m S_{ij'} \tag{2.2c}$$

$$H_4 = D_4 \sum_{\langle ijlmn \rangle} S_{ij}^{\dagger} P_l P_m P_n S_{ij'} \tag{2.2d}$$

where

$$D_1 = \frac{2t^2}{U - \Delta - 2V} \qquad D_{n+1} = \frac{V}{U - \Delta + (n-2)V} D_n \tag{2.2e}$$

from which it is evident that the two-particle interactions (represented in H_2) are repulsive.

Let us now consider the solution to the single-particle problem for this lattice. The basic conceptual difficulty is that the oxygen hole wants to be simultaneously in a singlet configuration with both of its neighbouring copper holes, and this is impossible. A simple description can only be achieved by considering states with local singlets (see figure 1). The problem with this description is that it is non-orthogonal. The state in figure 1(*a*) has probabilities 1 and 1/2 of being in a singlet with the left and right copper holes. The state in figure 1(*b*) is linearly independent with the probabilities reversed. These two states form a complete basis but have a non-trivial overlap.

There are several excitations which are easy to describe and which may be thought of as 'non-bonding'. In figure 1(*c*) three phase combinations of the four local singlet states connected to the central copper atom are shown. Any state that corresponds to a closed curve is an eigenstate of the Hamiltonian with zero hybridization energy. Several such states are depicted in figure 1(*d*). There is a natural separation of these states into those where the singlets are centred on the antiferromagnetic sublattice and those centred on the other sublattice. These states take care of three quarters of such states leaving the combination depicted in figure 1(*e*). In this limit the states of Zhang and Rice [13] can be justified, as also shown by Zhang [15]. All we need now is the Hamiltonian restricted to these states.

Denoting the uniform phase sum of figure 1(*e*) as $S_i^{\dagger}$ (the 'Zhang–Rice' singlet), we find that at the one-oxygen-hole level

$$H = -8\tilde{t} \sum_i S_i^{\dagger} S_i - \tilde{t} \sum_{\langle ii' \rangle \sigma} S_i^{\dagger} d_{i'\sigma} d_{i\sigma}^{\dagger} S_{i'} \tag{2.3a}$$

$$\tilde{t} = t^2/(U - \Delta - 2V) \tag{2.3b}$$

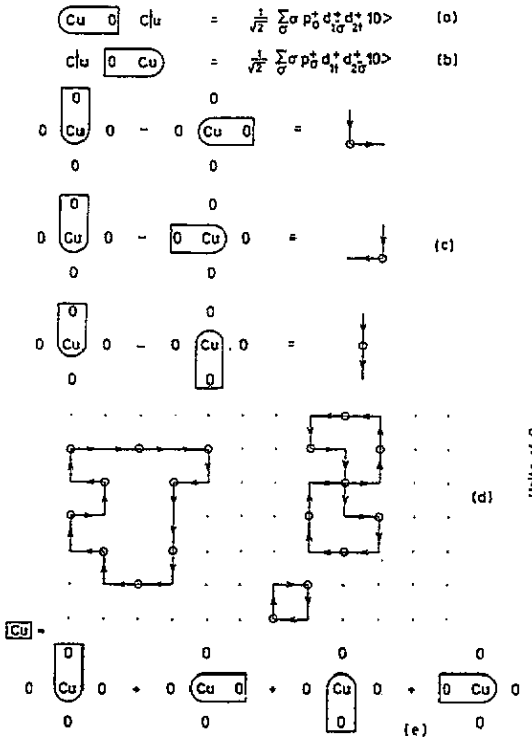

Figure 1. The Cu^{3+} limit with one mobile hole. (a), (b) The natural definitions for local singlets. (c) The non-bonding combinations of local singlets. (d) Various non-bonding eigenstates of the Cu^{3+} limit. (e) The bonding combination of local singlets.

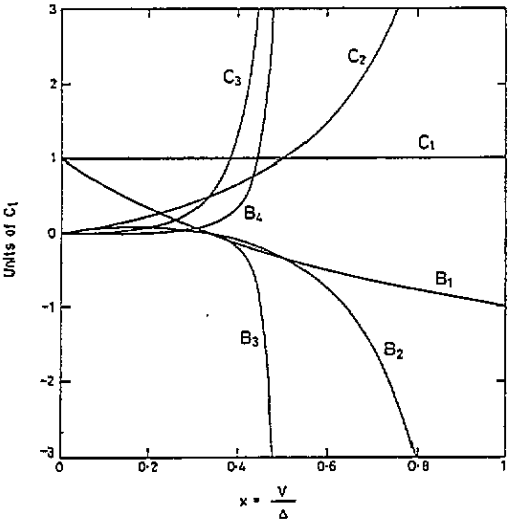

Figure 2. The relevant energy scales for the induced many-body interactions in this desciption. The subscript denotes the number of oxygen holes taking part in the interaction. The B and C denote the coefficients to the diagonal and off-diagonal terms, respectively.

where we *assume* that the $S_i^\dagger$s are orthogonal. The $S_i^\dagger$ may be considered as a 'vacancy' in the one-band Hubbard model in the strong-coupling limit. Indeed the spectrum is identical since the orthogonality matrix is invertible and the solutions to the problem in which the $S_i^\dagger$s are assumed orthogonal also diagonalize the non-orthogonal problem. The Nagaoka theorem [16] therefore holds, and the 'vacancy' spectrum of the ferromagnetic branch is

$$\epsilon_k = -8\tilde{t} - 2\tilde{t}[\cos(2k_x a) + \cos(2k_y a)] + \Delta/2 \tag{2.4}$$

with a ground state at $-12\tilde{t} + \Delta/2$ when $k = 0$.

Although at the one-particle level the spectrum is identical to that of the Hubbard model, it is noteworthy that at the two-particle level the non-orthogonality becomes important. This results in a nearest-neighbour repulsion between charge carriers, in addition to that resulting from the copper–oxygen repulsion.

3. Motion of holes via Cu^+ excitations: the basic behaviour of the Hamilitonian

When virtual double occupation of copper sites is excluded so that only virtual Cu^+ excitations are permitted, the order-t^2 Hamiltonian becomes, in the limit $U_p \to \infty$,

$$H = -t^2 \sum_{\langle ij \rangle} f_{ij}^{-1}(1 - P_j) + t^2 \sum_{\langle i;jj' \rangle \sigma\sigma'} p_{j'\sigma'}^\dagger d_{i\sigma}^\dagger \tilde{f}_{ijj'}^{-1} d_{i\sigma'} p_{j\sigma} \tag{3.1a}$$

$$f_{ij} = \Delta + V - V \sum_{\langle ijl \rangle} P_l \tag{3.1b}$$

$$\tilde{f}_{ijj'} = \Delta - V \sum_{\langle ijj'l \rangle} P_l. \tag{3.1c}$$

The inversion of f leads to the following terms in the Hamiltonian:

$$H_0 = -4A_1 \sum_i D_i \tag{3.2a}$$

$$H_1 = B_1 \sum_{\langle ij \rangle} D_i P_j + C_1 \sum_{\langle i;jj' \rangle \sigma\sigma'} d_{i\sigma}^\dagger d_{i\sigma'} p_{j'\sigma'}^\dagger p_{j\sigma} \tag{3.2b}$$

$$H_2 = B_2 \sum_{\langle i;jj' \rangle} D_i P_j P_{j'} + C_2 \sum_{\langle i;jj'k \rangle \sigma\sigma'} d_{i\sigma}^\dagger d_{i\sigma'} p_{j'\sigma'}^\dagger P_k p_{j\sigma} \tag{3.2c}$$

$$H_3 = B_3 \sum_{\langle i;jj'k \rangle} D_i P_j P_{j'} P_k + C_3 \sum_{\langle i;jj'kl \rangle \sigma\sigma'} d_{i\sigma}^\dagger d_{i\sigma'} p_{j'\sigma'}^\dagger P_k P_l p_{j\sigma} \tag{3.2d}$$

$$H_4 = B_4 \sum_{\langle i;jj'kl \rangle} D_i P_j P_{j'} P_k P_l \tag{3.2e}$$

where $\langle i; jj'k \rangle$ denotes that the three oxygen sites j, j' and k are all distinct and neighbour the copper site i, and that the sum runs over all permutations of the indices. The operators $d_{i\sigma}^\dagger$ and $p_{j\sigma}^\dagger$ create holes predominantly on the copper and oxygen sites, respectively, but with the optimal amount of hybridization onto neighbouring sites. The hole number operators are $D_i = \sum_\sigma d_{i\sigma}^\dagger d_{i\sigma}$ ($\equiv 1$) and $P_j = \sum_\sigma p_{j\sigma}^\dagger p_{j\sigma}$, respectively. Finally, the energy scales are

$$A_1 = \frac{t^2}{\Delta + V} \qquad A_{n+1} = \frac{V}{\Delta + V - nV} A_n \tag{3.3a}$$

$$B_1 = \frac{t^2(\Delta - 3V)}{\Delta(\Delta + V)} \qquad B_{n+1} = \frac{V}{\Delta - nV} B_n = A_{n+1} - (3 - n)A_{n+2} \tag{3.3b}$$

$$C_1 = \frac{t^2}{\Delta} \qquad C_{n+1} = \frac{V}{\Delta - nV} C_n = A_{n+1} + (1 + n)A_{n+2}. \tag{3.3c}$$

The structure of the Hamiltonian is shown in equation (3.2) where it has been decomposed into terms representing the number of charge carriers involved. There are two parts to each term. First, a diagonal part, with coefficient B, which represents the static energy of the copper spin and the surrounding oxygen holes. Second, an off-diagonal part, with coefficient C, which represents the hopping of an oxygen hole from one site to another in the presence of the copper spin and the relevant number of additional oxygen holes. The coefficients B and C are given in equation (3.3), and

plotted as a function of V/Δ in figure 2. The spin-independent terms have absolute magnitude, but the hole motion terms depend on the relative phase of the hole states.

We consider first the diagonal coefficients. Figure 2 shows that these terms are negative (attractive) when $V/\Delta > \frac{1}{3}$. This may be understood as follows: recall that the operator $d^{\dagger}_{i\sigma}$ creates a hole localized on a copper site which is maximally hybridized onto the neighbouring oxygen sites. The correction to the on-site energy of a 'copper' hole when there are no neighbouring oxygen holes is $-4t^2/(\Delta + V)$. The factor of 4 arises because there are four empty sites, and the denominator contains a V because during the virtual occupation of the oxygen site a repulsion from the neighbouring copper hole is experienced. Next, consider the correction to the on-site energy of a 'copper' hole when there is one neighbouring oxygen hole. This is $-3t^2/\Delta$. Since U_p is assumed large, one of the oxygen sites cannot be hybridized with, hence the factor 3. However, now the denominator is just Δ, because although the 'copper' hole experiences a repulsion from the neighbouring 'copper' hole during the virtual occupation of the oxygen site, it also *avoids* the repulsion arising from the presence of the oxygen hole. By similar arguments it is easy to show that the on-site energy corrections are $-2t^2/(\Delta - V)$ and $-t^2/(\Delta - 2V)$ for a 'copper' hole surrounded by two and three oxygen holes, respectively. If there are four oxygen holes surrounding a copper site, then the 'copper' hole cannot hybridize at all.

Now consider the energy difference between having two oxygen holes neighbouring the *same* copper site, and two separated oxygen holes. This is

$$-\frac{4t^2}{\Delta + V} - \frac{2t^2}{\Delta - V} + \frac{6t^2}{\Delta} = \frac{2t^2 V(\Delta - 3V)}{(\Delta - V)\Delta(\Delta + V)} \tag{3.4}$$

which is precisely B_2 (when summed over both permutations) and is negative when $V/\Delta > \frac{1}{3}$. The essential physics, which will reappear in other sections, is that during the hole's virtual vacation of the copper site, Coulomb repulsion is avoided. There is more Coulomb repulsion avoided if there are more oxygen holes surrounding the same copper site, hence leading to short-range attractive potentials. Clearly, $V/\Delta > \frac{1}{3}$ is an overestimate on the strength of V because of the blocking of occupied oxygen sites in the $U_p \to \infty$ limit.

Turning now to the off-diagonal terms, the matrix element to hop an oxygen hole from one site to another when there are n other holes present is $t^2/(\Delta - nV)$, or 0 if $n = 4$. Thus the amplitude of the matrix elements increases if there are more holes present. The reason is the same as above: Coulomb repulsion is avoided during the virtual Cu^+ excitation. This is of course the 'bare' matrix element and does not indicate the loss of kinetic energy resulting from occupied sites.

The question as to whether there are attractive channels for $V/\Delta \leqslant \frac{1}{3}$ depends on the sign acquired by the phase of the off-diagonal terms. This requires diagonalizing the Hamiltonian (3.2) which we address in the following sections.

The physics of the dominant interactions shown in figure 2 are clear. As the nearest-neighbour repulsion is increased there is a transition from a basically single-particle picture with weak two-particle interactions into a regime where three-particle interactions dominate. In section 4 we look at the three-particle regime involving clustering. When the single-particle energies dominate we expect the particles to delocalize and in the low-density limit the two-particle interactions will be the second most important interaction. In section 5 we consider this more realistic picture.

4. The clustering limit

In this section we analyse the behaviour of the Hamiltonian (3.2) in the limit where the three- and four-particle energy scales dominate. There is 'charge clustering' in this limit. The energy gain from delocalizing the holes is dominated by the short-range Coulomb effects, and bound states of several holes occur. We consider the questions of how many holes cluster together, and whether there are any residual dynamics.

There are some obvious physical questions to resolve before we proceed to a solution in this limit. Charge clustering is forbidden by the long-range nature of the Coulomb interaction, and so the effects that we are describing are to a certain extent 'unphysical'. Although long-range Coulomb interactions are omitted from a tight-binding description, because charge fluctuations are assumed screened, if this contribution were included it may not invalidate clustering on short length scales. On long length scales the charge remains homogeneous, while locally the charge clusters into either 'bubbles' or a sort of 'honeycomb' structure. If this picture is seriously considered then we must ask whether such a pattern could be dynamic, and hence lead to local charge fluctuations and a possible exotic type of superconductivity. We do not take these possibilities seriously, but the wealth of possible phenomena exhibited by our description deserves discussion.

There are two distinct types of clustering with a transition between these two types of behaviour when $2V = \Delta$. One type of clustering occurs when $2V > \Delta$ and results in a complete change of ground state. This is considered in section 4.1. The other type of clustering occurs when $2V$ approaches Δ from below, and is discussed in section 4.2. The behaviour at the transition, $2V = \Delta$, is pathological: the three- and four-body energy scales diverge and there appears to be a discontinuous change in hole density.

4.1. Static charge clustering: $2V > \Delta$

In this limit there is a static change in the ground state provided that there is a sufficient number of holes. Copper holes vacate their sites and reside on neighbouring oxygen sites in order to avoid the local Coulomb repulsion, V. These vacated copper sites cluster together, along with any added oxygen holes, to form a region of the lattice with singly occupied oxygen sites and vacant copper sites. Such a configuration obviously avoids the local repulsion, V, except at any boundary between regions. In a macroscopic cluster there are two holes per unit cell corresponding to one doped oxygen hole together with the original copper hole in the undoped phase. Comparing the energy per added hole in the macroscopic cluster to that of an isolated hole on an oxygen site immediately gives the criterion $2V = \Delta$ for the phase transition. This corresponds to the balance between the local Coulombic repulsion avoided and the loss from expelling a hole from a copper to an oxygen site.

This argument ignores boundary effects which would become important if the cluster were to split up into smaller droplets. Indeed, a droplet of six holes is only stable if $V > 3\Delta$, and a droplet of forty holes is only stable if $V > 5\Delta/6$.

Although this limit is not a physically realistic one, it illustrates the clustering of oxygen holes being driven by the copper–oxygen repulsion. In this case there is a static change of state from $Cu^{2+} \rightarrow Cu^{+}$. This transition arises because Coulomb repulsion between holes is avoided *provided* that the holes on oxygen sites cluster together. This result is a direct consequence of the unusual topology of the copper oxide planes in that copper sites have four neighbouring oxygen sites, whereas oxygen sites have only

two neighbouring copper sites. For smaller values of V the $Cu^{2+} \rightarrow Cu^{+}$ fluctuations are virtual. Nevertheless the same arguments apply; Coulomb repulsion is avoided if the oxygen holes cluster around the same copper site, implying short-range attractive potentials.

4.2. Dynamic charge clustering: $2V < \Delta$

As $2V$ aproaches Δ from below the three- and four-body terms dominate. There is a complication, however, in that the four-particle term is necessarily repulsive (in the large-U_p limit) and so the simple static picture of all the oxygen sites in some region being filled is invalid. There is a dynamic contribution to the energy, since the resonant energy is only saved when a copper site is surrounded by three oxygen holes. The physical source of this problem is easy to understand; if all four oxygen sites are occupied the copper hole is unable to move and so there is no virtual process to resonate.

Now, the static terms of (3.2) are independent of spin, but the dynamic terms depend on the spin coherence of the copper and oxygen holes. If we regard the resonant term as arising from the motion of vacancies in a background of holes, then by invoking the Nagaoka theorem [16] we can determine the spin coherence. Examination of the Hamiltonian (3.2*d*) shows that vacancy movement is unfrustrated, with negative hopping amplitude. The Nagaoka theorem then informs us that the maximum kinetic energy is gained (in the low-density limit) with a ferromagnetic spin background. Consequently, we restrict our attention to ferromagnetism, assuming that in a cluster of copper and oxygen holes all the spins are polarized.

The Hamiltonian (3.2*d*), (3.2*e*) then becomes

$$H = -A_4 \sum_{(i;jj'k)} P_j P_{j'} P_k + 3A_4 \sum_{(i;jj'kl)} p_j^{\dagger} P_k P_l p_{j'} + A_4 \sum_{(i;jklm)} P_j P_k P_l P_m. \quad (4.1)$$

This is not a particularly transparent representation and so we consider a description based around the cluster limit, where the number of holes is large and we may expand away from the case where each oxygen site has one hole. The excitations are now particle-like and we denote a particle by the creation operator $q_j^{\dagger}$. In terms of the new vacuum the Hamiltonian (4.1) is

$$H = -A_4 \sum_{(i;jklm)} [Q_j(1-Q_k)(1-Q_l)(1-Q_m) + 3q_j^{\dagger} q_k (1-Q_l)(1-Q_m)]. \quad (4.2)$$

This Hamiltonian is readily understood. Once the multiple counting of the terms has been extracted, we find that a single particle can move to any of the four oxygen sites surrounding a neighbouring copper site with hybridization $-6A_4$, provided that it is the only particle neighbouring that copper site.

The difficulty in solving (4.2) is deciding upon the local density of holes. If the holes cluster together and form a dense region then the representation (4.2) becomes the natural description. This Hamiltonian then describes the motion of vacancies in a cluster almost full of holes. If there were no vacancies there would be no contribution, and this is just the realization of the fact that a copper hole cannot move if all four neighbouring oxygen sites are full. In order to gain kinetic energy there must be vacancies, but how many? The cluster will assume a size that allows the optimal gain

in vacancy kinetic energy. To determine what this might be we consider the evidence from different clusters.

We have solved the cluster problems corresponding to the configurations depicted in figure 3. In order to compare the results we look at the gain per hole. For the plaquette of figure 3(*a*) there is one vacancy with an energy gain of $-8A_4$ per hole. For the two connected plaquettes of figure 3(*b*) there are two vacancies with a gain of $-8.4A_4$ per hole. The larger cluster is relatively stable. The star of five copper atoms (figure 3(*c*)) has four vacancies with a gain of $-8.3247A_4$ per hole. Finally, the square of figure 3(*d*) has four vacancies with an energy of $-9A_4$ per hole. Obviously the ground state will be a macroscopic cluster. The density of vacancies is probably not far from a value of half a hole per cell, and hence we would predict a discontinuity in the density of holes when $2V = \Delta$. The loop problems of figures 3(*e*)–(*h*) show the surprising result that the best solution is independent of the length of the loop at $-9A_4$. We postulate that this is also the infinite-loop result. Considering a square array of nine copper sites with the eight 'edge' sites considered as a loop and the central site as a 'perturbation' should immediately convince the reader that a more compact cluster is better than a loop.

It should be borne in mind that the gain in energy from extending the size of the cluster is minor and could easily be overcome, leading to a delocalized triple of holes. The long-range electrostatic energy prefers homogeneity of charge, so this contribution could easily be invoked to suggest delocalization. Indeed a picture of a homogeneous distribution of isolated lines of holes gaining $-9A_4$ energy per hole is an intriguing prospect of simultaneously ensuring local density fluctuations and global inhomogeneity of charge. These kinds of phase separation are reminiscent of the phase separation being suggested in the 't–J' model [17], although their origins are quite different.

There are two types of delocalization in this description. First, the motion of vacancies, $q_j^\dagger$, in a dense cluster of holes, and second the motion of isolated triples and the boundary of any cluster. The first effect seems very unlikely to lead to a superconducting instability, and it is only the second effect that needs to be seriously considered. Fluctuations in the boundary of any cluster are certainly charged and could, in principle, lead to superconductivity if there were long-range phase coherence which induces some form of gap. However, we do not believe that these limits have been realized in currently known experimental systems.

5. The delocalized limit

We now consider the limit that is easiest to justify experimentally. This is to assume that the nearest-neighbour Coulomb repulsion is much smaller than the charge transfer gap, $V \ll \Delta$.

Although we are predominantly interested in the two-particle interactions (3.2*c*) the 'single'-particle terms (3.2*b*) dominate in this limit. Furthermore, it is these terms (along with the superexchange term) which determine the underlying spin correlations. So, before proceeding to discuss the two-particle interactions we study one charge carrier first. As has been discussed elsewhere [18, 19], the motion of a single oxygen hole in the Cu^+ limit is rather subtle. Below we briefly analyse this in the $U_p \to \infty$ limit; a full account of the $U_p = 0$ limit is given in Barford [10].

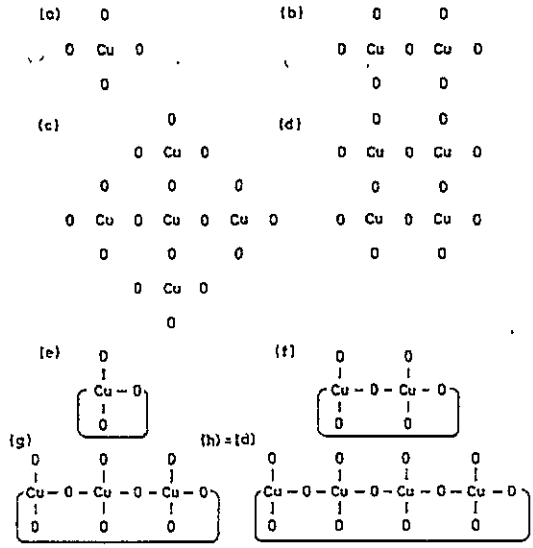

Figure 3. The configurations of atoms used to investigate the clustering limit. The 'loops' in figures (e)–(h) denote bonds forming periodic boundary conditions.

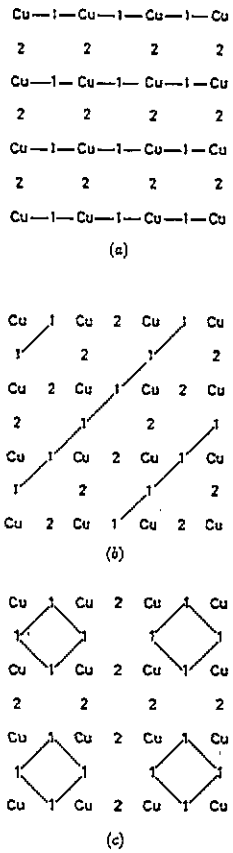

Figure 4. Several ways of breaking the oxygen atoms up into sublattices. (*a*) Two sublattices with pure square lattice symmetry. (*b*) Two sublattices that break the square lattice symmetry. Using standing waves composed from $\pm(\pi/2a)(1, 1)$, which reside on the non-interacting Fermi surface, we can isolate particles on one or other of the two sublattices. (*c*) Two sublattices where the 'squares' relevant for non-bonding orbitals play the dominant role.

The relevant Hamiltonian is (3.2*b*)

$$H_1 = B_1 \sum_{\langle ij \rangle} D_i P_j + C_1 \sum_{\{i;jj'\}\sigma} d^\dagger_{i\sigma} d_{i\sigma'} p^\dagger_{j'\sigma'} p_{j\sigma}. \tag{5.1}$$

The first term yields a constant energy for each oxygen hole provided that each copper site is occupied, so it is ignored. The ground and excited states are easily found for one plaquette (namely, a copper site surrounded by four oxygen sites). The ground state is a singlet spin configuration with the charge delocalized:

$$|S_i\rangle = \frac{1}{2\sqrt{2}} \sum_{j \in i\sigma} \mathrm{sgn}(\sigma) d^\dagger_{i\sigma} p^\dagger_{j\bar{\sigma}} |0\rangle \tag{5.2a}$$

with delocalization energy $-3C_1$. This corresponds to the 'Zhang–Rice' singlet [13]. The lowest-lying triplet excitation is triply degenerate:

$$|T_i\rangle = (1/\sqrt{2})d^\dagger_{i\sigma}(p^\dagger_{j\sigma} - p^\dagger_{j'\sigma})|0\rangle \tag{5.2b}$$

for some pair j, j' at the delocalization energy $-C_1$.

The problems emerge when we try to delocalize the hole on the lattice. A hole on an oxygen site is a nearest neighbour to two copper sites. Although it is possible for the oxygen spin to be simultaneously in a spin triplet with respect to these copper sites, and hence generate a ferromagnetic state, it is not possible to simultaneously make the oxygen spin singlet with respect to the two copper spins.

The purely ferromagnetic solution has the spectra as shown in equation (5.3), where $2a$ is the copper–copper spacing. In addition to the bonding band there is a non-bonding band at $-2C_1$:

$$\epsilon_k^{\text{non-bonding}} = -2C_1 \tag{5.3a}$$

$$\epsilon_k^{\text{bonding}} = -2C_1 + 2C_1\left[\cos(2k_x a) + \cos(2k_y a)\right]. \tag{5.3b}$$

Evidently, even restricting the local singlet to one plaquette gives a lower energy than the best ferromagnetic solution. At first sight we should therefore discard ferromagnetism and study more reasonable situations. We will not do this, however, for two reasons. First, if all the spins are parallel, then the copper spin system becomes passive and we may consider the charged oxygen system in isolation. This gives a way of separating the spin-fluctuation-induced many-body particle interactions from the direct charge-fluctuation-induced interactions. Second, by diagonalizing the two-body Hamiltonian around a single plaquette we derive the effective two-body potentials. We look at the two-particle interactions in the ferromagnetic state in section 5.1, and consider the low-spin scenario in section 5.2, summarizing in section 5.3.

5.1. Ferromagnetism

The two-particle interactions are now simply

$$H_2 = B_2 \sum_{\langle ijj'\rangle} P_j P_{j'} + C_2 \sum_{\langle ijj'k\rangle} p^\dagger_{j'} P_k p_j. \tag{5.4}$$

In the limit of interest, $A_1 > A_2 > A_3$, the first term is a repulsion between pairs of holes on the same plaquette. The question arises as to whether there a two-particle wavefunction for which the second term is attractive and dominates the first term.

In the diagonal representation the two-particle Hamilitonian is

$$H_2 = 4A_2 \sum_i \sum_{\mu=1}^{3} b^{i\dagger}_\mu b^i_\mu - 8A_3 \sum_i \sum_{\mu=1}^{3} c^{i\dagger}_\mu c^i_\mu \tag{5.5}$$

where

$$b^{i\dagger}_\mu = \tfrac{1}{2}(p^{i\dagger}_\alpha + p^{i\dagger}_\beta)(p^{i\dagger}_\gamma + p^{i\dagger}_\delta) \tag{5.6a}$$

$$c^{i\dagger}_\mu = \tfrac{1}{2}(p^{i\dagger}_\alpha - p^{i\dagger}_\beta)(p^{i\dagger}_\gamma - p^{i\dagger}_\delta) \tag{5.6b}$$

and where the sum i is over plaquettes and the indices $\{\alpha, \beta, \gamma, \delta\}$ label the different oxygen sites around the ith plaquette. The index μ corresponds to the three ways in which the four oxygen sites in the plaquette can split into two pairs, α, β and γ, δ.

Evidently, in a system with purely repulsive interactions we have found an attractive pairing. Pairs of holes in the $c_\mu^\dagger$ configuration feel an attraction with an eigenvalue of $-8A_3$, which corresponds to a coupling of ~ 0.5 eV, using the data in section 1.

The dominant effect is a repulsion between a pair made up of a hole in phase on one pair of sites and another hole in phase on the other pair of sites. The weaker attractive combination is the antiphase combination of the two holes. If we consider $c_\mu^\dagger$ as a Cooper pair, then we may deduce something about the symmetry of the superconducting gap function.

Let us now reconstitute the lattice. If we consider the two-particle interaction in isolation, then the natural Cooper pair has one member on one oxygen sublattice and the other member on the other sublattice. Since the pairs have parallel spins the spin symmetry is symmetric. The sublattice degree of freedom is antisymmetric and so the final spatial symmetry is therefore symmetric. Three ways of assigning sublattice indices are shown in figure 4. Pairs moving parallel to the Cartesian axes would favour the situation depicted in figure 4(a). Holes with a uniform wavefunction would feel the repulsion mediated by $b_\mu^\dagger$, whereas holes with alternating phase would feel the attraction mediated by $c_\mu^\dagger$. A similiar situation holds in figure 4(b). Figure 4(c) shows holes on the 'squares' interacting with each other. The relevant situation to consider is that corresponding to holes at the Fermi surface, for these can make use of the weak attractive interaction at little loss in kinetic energy. However, there is a complication as the lowest band in the ferromagnetic bandstructure is flat, and so there is an implied degeneracy. The kinetic energy is optimized using the non-bonding band. Inspection of the non-bonding solutions resolves the predicament. We observe that a single hole delocalized on one of the 'squares' in figure 4(c) with an alternating phase around the 'square' is an eigenstate of the Hamiltonian, and corresponds to a real-space non-bonding orbital. The alternating phase is perfect for gaining the two-body attraction and so we find that the ground state for the ferromagnet, with weak two-body interactions included, is composed of localized non-bonding states clustered together in a pattern similar to figure 4(c). However, this is still not a scenario for superconductivity as the states are localized.

There are bonding states that are degenerate with the non-bonding states; those for which $\gamma_k = \pm(\pi/2a)(1,1)$. These states have precisely the alternating symmetry of figure 4(b) and so could conceivably carry current. A close inspection of the wavefunction shows that 's-wave' pairs suffer the repulsion while the 'd-wave' pairs feel the weak attraction.

5.2. *Low spin*

For three spins the low-spin scenario is total spin $\frac{1}{2}$. We analyse this case to try to deduce the sort of Cooper pair to be expected in a low-spin ground state.

The 'two'-particle interactions are

$$H_2 = B_2 \sum_{(ijj')} D_i P_j P_{j'} + C_2 \sum_{(ijj'k)} d_{i\sigma}^\dagger d_{i\sigma'} p_{j'\sigma'}^\dagger P_k p_{j\sigma}. \tag{5.7}$$

In a total spin $\frac{1}{2}$ subspace the diagonalized Hamiltonian is

$$H_2 = 4A_4 \sum_i \sum_{\mu=1}^{4} e_\mu^{i\dagger} e_\mu^i + (3A_2 - 2A_3) \sum_i \sum_{\mu=1}^{3} f_\mu^{i\dagger} f_\mu^i$$
$$+ (A_2 - 6A_3) \sum_i \sum_{\mu=1}^{2} g_\mu^{i\dagger} g_\mu^i - (A_2 - 10A_3) \sum_i \sum_{\mu=1}^{3} h_\mu^{i\dagger} h_\mu^i. \tag{5.8}$$

Again we find an attractive channel, now corresponding to the $h_\mu^{i\dagger}$ combination

$$h_\mu^{i\dagger} = \frac{1}{\sqrt{10}}\left[(p_{\alpha\uparrow}^{i\dagger} + p_{\beta\uparrow}^{i\dagger})(p_{\gamma\uparrow}^{i\dagger} + p_{\delta\uparrow}^{i\dagger})d_{i\downarrow}^\dagger - \frac{1}{2}\sum_\sigma (p_{\alpha\sigma}^{i\dagger} + p_{\beta\sigma}^{i\dagger})(p_{\gamma\bar{\sigma}}^{i\dagger} + p_{\delta\bar{\sigma}}^{i\dagger})d_{i\uparrow}^\dagger\right]$$
$$+ \frac{1}{\sqrt{5}}\left[\frac{1}{\sqrt{2}}\sum_\sigma \mathrm{sgn}(\sigma) p_{\gamma\sigma}^{i\dagger} p_{\delta\bar{\sigma}}^{i\dagger} - \frac{1}{\sqrt{2}}\sum_\sigma \mathrm{sgn}(\sigma) p_{\alpha\sigma}^{i\dagger} p_{\beta\bar{\sigma}}^{i\dagger}\right] d_{i\uparrow}^\dagger \tag{5.9a}$$

and, as before, $\{\alpha, \beta, \gamma, \delta\}$ labels the oxygen sites, and the index μ runs over the possible ways of splitting the sites into pairs. There is another representation for this quantity that is not orthogonal but that is very suggestive:

$$h_\mu^{i\dagger} \doteq \frac{1}{2\sqrt{5}}\left[(p_{\alpha\uparrow}^{i\dagger} + p_{\beta\uparrow}^{i\dagger})\frac{1}{\sqrt{2}}\sum_\sigma \mathrm{sgn}(\sigma)(p_{\gamma\sigma}^{i\dagger} + p_{\delta\sigma}^{i\dagger})d_{i\bar{\sigma}}^\dagger\right.$$
$$\left. - (p_{\gamma\uparrow}^{i\dagger} + p_{\alpha\uparrow}^{i\dagger})\frac{1}{\sqrt{2}}\sum_\sigma \mathrm{sgn}(\sigma)(p_{\alpha\sigma}^{i\dagger} + p_{\beta\sigma}^{i\dagger})d_{i\bar{\sigma}}^\dagger\right]$$
$$+ \frac{1}{\sqrt{5}}\left[p_{\alpha\uparrow}^{i\dagger}\frac{1}{\sqrt{2}}\sum_\sigma \mathrm{sgn}(\sigma) p_{\beta\sigma}^{i\dagger} d_{i\bar{\sigma}}^\dagger + p_{\beta\uparrow}^{i\dagger}\frac{1}{\sqrt{2}}\sum_\sigma \mathrm{sgn}(\sigma) p_{\alpha\sigma}^{i\dagger} d_{i\bar{\sigma}}^\dagger\right.$$
$$\left. - p_{\gamma\uparrow}^{i\dagger}\frac{1}{\sqrt{2}}\sum_\sigma \mathrm{sgn}(\sigma) p_{\delta\sigma}^{i\dagger} d_{i\bar{\sigma}}^\dagger - p_{\delta\uparrow}^{i\dagger}\frac{1}{\sqrt{2}}\sum_\sigma \mathrm{sgn}(\sigma) p_{\gamma\sigma}^{i\dagger} d_{i\bar{\sigma}}^\dagger\right]. \tag{5.9b}$$

From this representation it is clear that the local singlet pairs of one copper and one oxygen hole are all in phase, while the '↑' contributions are in opposite phases on the two 'sublattices'.

Let us now consider the symmetry of the 'Cooper pairs'. The object $h_\mu^\dagger$ does not create a pair of particles, but a triple. The important point, however, is that only two of these particles, the oxygen holes, display a charge degree of freedom. The copper hole displays only a spin degree of freedom and so, although it participates in the spin symmetry of the Cooper pair, it does not stop the object being doubly charged, and does not participate directly in the motion of the pair. Considering the two oxygen holes to be the pair and the copper hole to be a 'sink' for 'unwanted quantum numbers' we find that the pair has mixed character. The natural separation when the lattice is reconstituted is again into the two sublattices. We find, from (5.9*a*), that two fifths of the wavefunction has the pair in a relative singlet with symmetric sublattice coupling and symmetric spatial symmetry, while the other three fifths has the pair in a relative triplet with antisymmetric sublattice coupling and symmetric spatial symmetry. This predicts an 's-wave' spatial gap function.

The final issue to deal with concerns the relation between the single-particle solutions and the pairing interactions. Are the holes at the Fermi surface of the

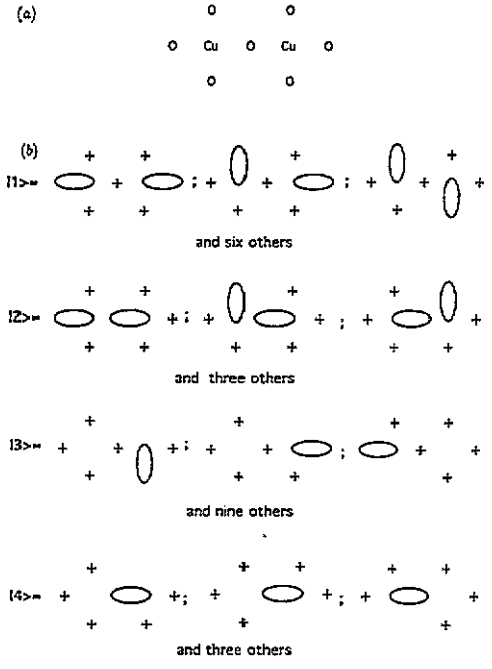

Figure 5. (*a*) The configuration of atoms chosen to investigate the two-oxygen-hole wavefunction in the absence of nearest-neighbour repulsion. (*b*) A pictorial representation of the symmetries of the states that form the basis described in the text.

correct symmetry to make use of this attraction? For the ferromagnetic case this was easy; an analysis of the low lying single-particle wavefunction showed that the local symmetry was precisely that of the combinations making up the Cooper pairs. We do not have the exact single-particle wavefunctions for the low-spin case, so approximate arguments are necessary.

In order to determine the local correlations in more detail we performed a ground state calculation for two oxygen holes on the cluster of figure 5(*a*) using the 'single'-particle Hamiltonian (5.1). The ground state is a total spin singlet, with the four states pictured in figure 5(*b*) forming a basis. It is found that the ground state is predominantly $|1\rangle$ and $|2\rangle$ with a small admixture of $|3\rangle$. The eigenvalue is $-5.6613C_1$ to be compared with the unfrustrated bound of $-6.0C_1$. The important comparison is between $|2\rangle$ and $|3\rangle$, which have both holes neighbouring the copper site, and the state described by $h_\mu^\dagger$. There is no *a priori* reason for the present wavefunction to be related to $h_\mu^\dagger$, but there is a strong resemblance. The phases are such that all the singlets of copper and oxygen holes are in phase, and the hole on the central oxygen site in $|2\rangle$ is in antiphase with the non-singlet contributions in $|3\rangle$. This is the closest wavefunction to $h_\mu^\dagger$ which can be made with the restricted symmetry. The dominant central hole is antiphase with the two elements of the other sublattice, in agreement with (5.9*b*).

5.3. Discussion

Let us now consider whether or not the attractive channels found in the above discussions are relevant to the full many-body problem. Since we cannot solve this problem exactly the discussion will necessarily be rather general.

In the weak-coupling limit the Hamiltonian (3.2) is

$$H = H_1 + H_2 \tag{5.10}$$

with H_1 given by (5.1) and H_2 by (5.7). Now, H_1 is the dominant term, and implicitly contains many-body interactions which cannot be solved. H_2, however, can be solved and contains explicit interactions. The question is, are these interactions sympathetic to those of H_1? To analyse this let us write H_2 as

$$H_2 = \sum_i H_2^{(i)} \tag{5.11}$$

where the sum is over all plaquettes. $H_2^{(i)}$ can be readily diagonalized, as shown in sections 5.1 and 5.2. We therefore write

$$H = H_1 + \sum_i \sum_{\mu=1}^{18} \epsilon_\mu X_\mu^{i\dagger} X_\mu^i \tag{5.12}$$

where ϵ_μ is the eigenvalue that corresponds to the eigenfunction $|X_\mu^i\rangle = X_\mu^{i\dagger}|0\rangle$. The operator $X_\mu^{i\dagger}$ creates the 'Cooper pairs' of equations (5.6) and (5.9). There are four negative eigenvalues (attractive channels) and fourteen positive ones (repulsive channels). These may be regarded as being short-range attractive and repulsive two-body potentials.

Since H_1 is the dominant term we need to consider which symmetry (two oxygen hole correlations about the same plaquette) this term prefers. If its ground state wavefunction has correlations described by an $|X_\mu\rangle$ with a negative eigenvalue, then H_2 automatically acts as an attractive potential, and *vice versa*. For the ferromagnetic case we showed that the wavefunction associated with H_1 had precisely the right correlations to experience the attractive potential. This was confirmed for the low-spin case by the calculation on the cluster of two neighbouring plaquettes.

The full many-body eigenstate of (5.12) will, in general, contain superpositions of all the basis states which span the Hilbert space. These basis states will, in turn, have as components the $|X_\mu\rangle$s. From the previous discussion, we expect these terms to be dominated by the attractive channels. Although we cannot state the precise symmetry of the Cooper pairs, as they will be superpositions of the $X_\mu^\dagger$s, the cluster calculation suggests that if the total spin of the complete many-body wavefunction is zero then the Cooper pair will be spatially symmetric. In the high-temperature superconductors the motion of the holes coupled to the Heisenberg term has a dominant effect, destroying long-range magnetic correlations and guaranteeing that the total spin is in a total spin singlet. This calculation therefore lends evidence to the suggestion that the charge fluctuations coupled to the Coulomb repulsion result in 's-wave' pairing.

6. Conclusions

The copper oxide systems are characterized by charge transfer resonances due to the proximity of the atomic copper and oxygen energy levels. These charge fluctuations, coupled to the nearest-neighbour copper–oxygen repulsion, V, have been investigated by deriving effective Hamiltonians which describe the low-energy behaviour, starting from the generic two-band model. We considered hole doping only.

When $Cu^{2+} \rightarrow Cu^{3+}$ fluctuations dominate we find a description in which the oxygen hole forms a singlet with the copper spin. This entity propagates through the

square lattice like a vacancy in a single-band Hubbard model. This is equivalent to the description of Zhang [15]. The effect of the copper–oxygen repulsion is to cause a nearest-neighbour repulsion between these singlets. The reason for this repulsion is that during the oxygen hole's virtual occupation of the copper site it feels a repulsion from all the oxygen holes neighbouring that copper site.

If $Cu^{2+} \rightarrow Cu^{+}$ fluctuations dominate, however, we have shown that short-range Coulomb repulsion can give rise to attractive interactions between some of the charge carriers in the system. This is because during the 'copper' hole's virtual vacation of its site and occupation of a neighbouring oxygen site it avoids the repulsion from all the oxygen holes neighbouring that copper site.

The overall behaviour is governed by the ratio of the copper–oxygen repulsion to the charge transfer gap, V/Δ. When $0 \ll V/\Delta \leqslant \frac{1}{2}$, we proved that charge clustering takes place by showing that clusters of charge are more stable than isolated charges. On the other hand, when $0 \leqslant V/\Delta \ll \frac{1}{2}$, the single-particle terms dominate and the question of whether weak-coupling superconductivity exists is a subtle one which we have not been able to address unambiguously. As we discussed in detail in section 5.3, the Hamiltonian contains both attractive and repulsive short-range two-body potentials. The holes at the Fermi surface will only experience the attractive potentials if they have correlations consistent with them; otherwise the repulsive interactions will act. On a small cluster we showed that the correlations are consistent with the attractive potentials, and indicate 's'-wave pairing. Experimentally, V/Δ would appear to be about 1/4, placing the copper oxide systems in the weak-coupling limit.

Finally, let us recall the approximations made in these calculations. We derived an effective Hamiltonian of $O(t^2)$, thereby neglecting spin fluctuations. The copper and oxygen Coulomb repulsions were assumed very large, which forbids double occupation of copper and oxygen sites. The latter constraint is probably too severe, and tends to work against the attractive mechanisms operative here. Lastly, the direct oxygen–oxygen hybridization was neglected.

Appendix

The analysis of section 2 is completed by inverting the operator $f_{ij\sigma}$ of equation (2.1*c*). The solution may be deduced from the more general problem

$$F = \left[A - a_i \sum_{i=1}^{N} P_i\right]^{-1} \tag{A1}$$

where the P_i are mutually commuting projection operators:

$$P_i^2 = P_i. \tag{A2}$$

Obviously $d_{i\sigma}^{\dagger} d_{i\sigma}$ and $p_{j\sigma}^{\dagger} p_{j\sigma}$ are projection operators, but if double occupancy is prohibited then $D_i = \sum_{\sigma} d_{i\sigma}^{\dagger} d_{i\sigma}$ is effectively a projection operator since

$$D_i^2 - D_i = 2 d_{i\sigma}^{\dagger} d_{i\bar{\sigma}}^{\dagger} d_{i\bar{\sigma}} d_{i\sigma} \tag{A3}$$

and the right-hand side only contributes when a site is doubly occupied.

We may invert the operators iteratively by observing that

$$F = (1 - P_1)\left[A - a_i \sum_{i=2}^{N} P_i\right]^{-1} + P_1\left[A - a_1 - a_i \sum_{i=2}^{N} P_i\right]^{-1} \tag{A4}$$

and hence

$$F = \sum_{I} \left(A - \sum_{i \in I} a_i\right)^{-1} \prod_{i \in I} P_i \prod_{j \in I} (1 - P_j) \tag{A5}$$

where I denotes all the subsets of $\{1, 2, \ldots, N\}$.

A final result which is of use in deriving the forms presented in section 4 is

$$\left[A - V \sum_{i=1}^{N} P_i\right]^{-1} = A_0 + A_1 \sum_{i_1=1}^{N} P_{i_1} + A_2 \sum_{i_1 i_2} P_{I_1} P_{i_2} + A_3 \sum_{i_1 i_2 i_3} P_{i_1} P_{i_2} P_{i_3} \ldots \tag{A6}$$

where

$$A_n = [V/(A - nV)]A_{n-1} \qquad A_0 = 1/A \tag{A7}$$

and $\{i_1 i_2 i_3\}$ denotes mutually exclusive labels including all permutations.

References

[1] Varma C M, Schmitt-Rink S and Abrahams E 1987 *Solid State Commun.* **62** 681
[2] Hirsch J E 1987 *Phys. Rev. Lett.* **58** 228
[3] Balseiro C A, Rojo A G, Gagliano E R and Alascio B 1988 *Phys. Rev.* B **38** 9315
[4] Littlewood P B, Varma C M, Schmitt-Rink S and Abrahams E 1989 *Phys. Rev.* B **39** 12371
[5] Grilli M, Raimondi R, Castellani C, Di Castro C and Kotliar G 1991 *Int. J. Mod. Phys.* B **5** 309; 1991 *Phys. Rev. Lett.* **67** 259
[6] Emery V J 1987 *Phys. Rev. Lett.* **58** 2794
[7] Sawatzky G A 1992 *High Temperature Superconductivity* ed D P Tunstall and W Barford (Bristol: Adam Hilger)
[8] McMahan A K, Martin R M and Satpathy S 1988 *Phys. Rev.* B **38** 6650
[9] Schrieffer J R and Woolf P A 1966 *Phys. Rev.* B **149** 491
[10] Kittel C 1963 *Quantum Theory of Solids* (New York: Wiley)
[11] Fedro A J and Schüttler H-B 1989 *Phys. Rev.* B **40** 5155
[12] Long M W and Barford W 1989 *Rutherford Appleton Laboratory Report* RAL-89-053/4
[13] Zhang F C and Rice T M 1988 *Phys. Rev.* B **37** 3579
[14] Long M W and Barford W 1989 *Physica* C **162–4** 789
[15] Zhang F C 1988 *Phys. Rev.* B **37** 3759
[16] Nagaoka Y 1966 *Phys. Rev.* **147** 392
[17] Emery V J, Kivelson S and Lin H Q 1990 *Phys. Rev. Lett.* **64** 475
[18] Long M W 1988 *J. Phys. C: Solid State Phys.* **21** L939
[19] Barford W 1990 *J. Phys.: Condens. Matter* **2** 2965